Cardiovascular Toxicology (2021) 21:322–335
https://doi.org/10.1007/s12012-020-09622-1

Interrelated In Vitro Mechanisms of Sibutramine-Induced Cardiotoxicity

Feyza Alyu[1] · Yusuf Olgar[2] · Sinan Degirmenci[2] · Belma Turan[2,3] · Yusuf Ozturk[1]

Received: 15 August 2020 / Accepted: 24 November 2020 / Published online: 3 January 2021

Abstract

Consumption of illicit pharmaceutical products containing sibutramine has been reported to cause cardiovascular toxicity problems. This study aimed to demonstrate the toxicity profile of sibutramine, and thereby provide important implications for the development of more effective strategies in both clinical approaches and drug design studies. Action potentials (APs) were determined from freshly isolated ventricular cardiomyocytes with whole-cell configuration of current clamp as online. The maximum amplitude of APs (MAPs), the resting membrane potential (RMP), and AP duration from the repolarization phases were calculated from original records. The voltage-dependent K^+-channel currents (I_K) were recorded in the presence of external Cd^{2+} and both inward and outward parts of the current were calculated, while their expression levels were determined with qPCR. The levels of intracellular free Ca^{2+} and H^+ (pH_i) as well as reactive oxygen species (ROS) were measured using either a ratiometric micro-spectrofluorometer or confocal microscope. The mechanical activity of isolated hearts was observed with Langendorff-perfusion system. Acute sibutramine applications (10^{-8}–10^{-5} M) induced significant alterations in both MAPs and RMP as well as the repolarization phases of APs and I_K in a concentration-dependent manner. Sibutramine (10 µM) induced Ca^{2+}-release from the sarcoplasmic reticulum under either electrical or caffeine stimulation, whereas it depressed left ventricular developed pressure with a marked decrease in the end-diastolic pressure. pH_i inhibition by sibutramine supports the observed negative alterations in contractility. Changes in mRNA levels of different I_K subunits are consistent with the acute inhibition of the repolarizing I_K, affecting AP parameters, and provoke the cardiotoxicity.

Keywords Sibutramine · Patch-clamp techniques · Langendorff-perfused heart · Reactive oxygen species · Fluorescence microscopy

Abbreviations

SBT	Sibutramine
LV	Left ventricular
I_K	Voltage-dependent K^+-channel currents
ROS	Reactive oxygen species
AP	Action potential
MAP	Maximum amplitude of AP
RMP	Resting membrane potential
APD	Action potential duration
APD25	Action potential duration at 25% completion of repolarization
APD50	Action potential duration at 50% completion of repolarization
APD75	Action potential duration at 75% completion of repolarization
APD90	Action potential duration at 90% completion of repolarization
I_{to}	Transient outward K^+ currents
I_{ss}	Steady-state current
I_{K1}	Inward rectifier K^+ current
$[Ca^{2+}]_i$	Intracellular Ca^{2+} level
TP	Time to peak
LVESP	Left ventricular end-systolic pressure
LVEDP	Left ventricular end-diastolic pressure
DT50	Left ventricular half-relaxation time

Handling editor: Rajiv Janardhanan.

Feyza Alyu and Yusuf Olgar have contributed equally.

✉ Yusuf Ozturk
yozturk1958@gmail.com

[1] Department of Pharmacology, Faculty of Pharmacy, Anadolu University, Yunus Emre Campus, 26470 Eskisehir, Turkey

[2] Department of Biophysics, Faculty of Medicine, Ankara University, 06230 Ankara, Turkey

[3] Department of Biophysics, Faculty of Medicine, Lokman Hekim University, 06230 Ankara, Turkey

Introduction

Sibutramine (SBT), an anorexic agent, has been a commonly abused illicit drug for the purpose of rapid weight loss, although its therapeutic use has been banned because of its cardiovascular safety issues. Food and Drug Administration report has displayed that even at minimal effective doses, SBT caused many cardiovascular side effects and deaths [1]. Being a predisposing factor for cardiovascular diseases, obesity is an epidemic. Weight loss is the first stage for controlling or obviation of the clinical outcomes of obesity. Unfortunately, adequate weight loss cannot be achieved and maintained with exercise and diet generally [2–4]. Therefore, obese patients seek a potent remedy to lose weight in non-prescription medicines. SBT is included in some of non-prescription medicines and health foods and counterfeit drugs or slimming products.

By and large, it is accepted that there is a close relationship between weight loss and improvement in health by reducing cardiovascular risk factors [5]. However, the SBT Cardiovascular Outcomes study has pointed out that patients with high risk of cardiovascular disease exhibit elevated cardiovascular morbidity (non-fatal acute myocardial infarction and non-fatal stroke) without an increase in mortality [2]. In addition, the consumption of illicit pharmaceutical products containing SBT has been reported to cause cardiovascular crisis [1]. Also, taking into consideration the relation between obesity and the development of hemodynamic alterations, Zannand et al. [6] have treated obese subjects with SBT for 6 months and investigated the parameters of the heart such as left ventricular (LV) wall stress and hypertrophy. For those obese patients, SBT has not been found to alter heart valves, ventricular dimensions, and electrocardiogram variables. However, those studies have no attempt to assess any potential effect of SBT regarding electrophysiological parameters of the heart at the cellular level, whether this can modify the entire cardiovascular risk profile.

Therefore, understanding the mechanism of SBT cardiotoxicity is important mostly to develop more specific strategies for the clinical management of cardiac manifestations due to its illicit or legal ongoing use [7, 8] but also for developing agents being effective for the treatment of obesity without inducing these particular mechanisms and having a safer profile. Discovering the mechanisms will fulfill the necessity to determine several test parameters for toxicity while evaluating both the derivatives of SBT and other candidates in drug development studies as antiobesity drugs. Investigating cardiological parameters on rat cardiomyocytes is a commonly used method to obtain data that affect clinical approaches. In the present study, exposure to SBT may alter expressions of different subunit voltage-dependent K^+-channel current (I_K) genes, electrophysiological parameters, in vitro mechanical activity, intracellular levels of pH, free Ca^{2+} and reactive oxygen species (ROS) levels, which are all interrelated and potentially participate to the adverse clinical outcomes [9–12].

Methods

Animals and Isolation of Ventricular Myocytes

6-month-old drug or test naïve male Wistar rats weighing 250–300 g were used. Storage room conditions for the animals were a constant temperature (23 ± 2 °C), illumination (12-h light/dark cycles), and relative humidity (50 ± 10%). Rats were fed ad libitum with standard chow and had free access to drinking water. The number of rats per cage, with bedding material as sawdust, was 5.

To isolate cardiomyocytes freshly, anesthesia was performed with sodium pentobarbital (50 mg/kg, i.p., the depth of the anesthesia was observed via firm toe pinch) and hearts were excised rapidly. The aorta was cannulated on a Langendorff apparatus and perfused retrogradely through the coronary arteries with a Ca^{2+}-free solution at 37 °C. Afterward, a perfusion was performed and digestion of the hearts was achieved through using the same solution containing 0.07 mg/ml protease (Sigma type XIV) and 0.8 mg/ml collagenase (Collagenase A, Roche) for 20 min. After removal, LV was cut into small pieces and gently massaged through a nylon mesh. Afterward, the cell suspension was washed multiple times and an increase in Ca^{2+} concentration was performed through a gradual way to a final concentration of 1.3 mM. Then, this solution was used to keep the cells at 37 °C. 1 h following the isolation of the cells, experiments were carried out at room temperature [13, 14]. Solely Ca^{2+}-tolerant single rod-shaped cells with clear edges plus no spontaneous contractions were used for the experiments [15].

The freshly isolated cardiomyocytes incubated for 3 h with sibutramine together with untreated controls. At the end of the incubation, all samples were quickly frozen and kept in − 80 °C until the day of experiments.

Solutions and Chemicals

Perfusion solutions for action potential (AP) recordings (in mM: 1.2 $MgSO_4$, 137 NaCl, 1.2 KH_2PO_4, 5.4 KCl, 20 glucose, and 6 HEPES, at pH 7.2 adjusted with NaOH, bubbled with 100% O_2) were freshly prepared in each experiment day. Cells were superfused with normal Tyrode's solution (in mM): 1.5 $CaCl_2$, 11.8 HEPES, 5.4 KCl, 137 NaCl, 0.5 $MgCl_2$, 10 glucose, pH 7.40 adjusted with NaOH.

Solution prepared for recording of the K^+ currents was prepared accordingly: for the pipette (mM): 130 KCl, 5 MgATP, 10 Na-HEPES, 10 NaCl (pH 7.2 adjusted with CsOH). Besides, to block the Ca^{2+} currents, 250 µM $CdCl_2$ was included in the intracapillary environment. Solution in the pipette for AP recordings included (in mM): 20 HEPES, 120 KCl, 5 Na_2ATP, 6.8 $MgCl_2$, 10 EGTA, 0.4 Na_2GTP, 4.7 $CaCl_2$ (pH 7.4 adjusted with CsOH).

The perfusion medium for experiments with Langendorff-perfused hearts contained 1.0 mM $CaCl_2$, 119 mM NaCl, 1.2 mM KH_2PO_4, 4.8 mM KCl, 1.2 mM $MgSO_4$, 10 mM glucose, and 20 mM $NaHCO_3$. This solution was gassed with 95% O_2/5% CO_2 and maintained at 37 °C, at pH 7.4 adjusted with NaOH.

All chemicals used were purchased from Sigma (Sigma-Aldrich Chemie, Steinheim, Germany/St. Louis, MO, USA) unless otherwise stated. 3.34 mg SBT (Cayman Chemicals, Ann Arbor, Michigan USA) was dissolved in 500 µL DMSO as a vehicle to prepare a 5×10^{-3} M stock solution, and 20 µL aliquots were frozen and, before the experimental period, diluted with an external solution to a final concentration of 10^{-4} M. Afterwards, dose range between 10^{-5} and 10^{-8} M was applied in a concentration-dependent manner. Based on previous reports related to DMSO effects on cells [16–18], the final amount of DMSO was adjusted to a concentration not greater than 0.3% (v/v).

Here, 1 and 10 µM SBT pretreatment was assessed in most of the experiments and hence SBT is displaying statistically significant effects mainly at these concentrations on electrophysiological parameters tested in this study.

Recording of AP and K^+ Currents

Recording of the current was performed by the whole-cell configuration of the patch-clamp amplifier (Axon200B, Molecular Devices, USA). Changes in the AP amplitude and resting membrane potential (RMP) were acquired from the division of the currents to cell capacitance. The frequency for AP recordings is 1 Hz. The electrode resistance value was 2–2.5 MΩ. For recording, injections of small depolarizing pulses to the cell were carried out within current-clamping configuration, the cell was excited, and changes in membrane potential were monitored. The AP durations (APD) to 25% (APD_{25}), 50% (APD_{50}), 75% (APD_{75}), and 90% (APD_{90}) of repolarization were analyzed.

K^+ currents were obtained with the whole-cell configuration of the voltage-clamp method using step protocols. For evoking K^+ currents, 3-s test pulses starting from a holding potential of − 70 mV and depolarizing steps with 10 mV increments in between − 120 and + 70 mV were applied. Subtraction of the current values at the end of the 3 s pulse from the peak values was used to calculate the transient outward K^+ currents (I_{to}). Current values at the end of the 3-s pulse are also described as steady-state current (I_{ss}). Afterward, determined current values were divided by cell capacity and introduced as current density, pA/pF [19]. The inward rectifier K^+ current, I_{K1}, was assessed by measuring current amplitudes in response to steps to membrane potentials negative to I_{ss} activation (− 50 to − 120 mV) [16]. The data were analyzed and collected using Clampfit software and pCLAMP (Version 9, Axon Instruments, USA), respectively.

qPCR Measurements

RNA Isolation Kit (740955.10; Macherey-Nagel) was utilized for total RNA preparation. Purified total RNA was reverse transcribed with a ProtoScript First Strand cDNA Synthesis Kit (E6300S; New England Biolabs). Quantification of the first-strand cDNAs was performed with GoTaq qPCR Master Mix (A6001; Promega). Through the National Center for Biotechnology Information and Ensembl databases, extents of the amplified fragment PCR products regarding each of the primers and specificity of all primers were checked. Primer sequences for Kv4.3, Kv4.2, Kv2.1, Kv1.4, and Cyclophilin are listed in Table 1. Analysis of the fold changes in the genes was carried out through the comparative ($2^{-\Delta\Delta Ct}$) method.

Determination of Cellular Free Ca^{2+} Level in Cardiomyocytes

Intracellular Ca^{2+} transients were measured by Fura-2 fluorescence at room temperature (21 ± 2 °C). Basal and transient changes of cellular (intracellular) Ca^{2+} level ($[Ca^{2+}]_i$) in cells loaded with Fura-2AM (3 µM for 40 min at 37 °C) were assessed by a ratiometric fluorescence recording system

Table 1 Primer sequences for Cyclophilin, Kcnd3, Kcnd2, Kcnb1, and Kcna4

Primers	Sense (5′–3′)	Antisense (5′–3′)
Kcnd3	GACCACTCTGGAGCGCTATC	TCATAGCGTGGGTAGTGCAG
Kcnd2	CTTCACTATCCCCGCCAT	GTTTCCACCACATTCGCG
Kcnb1	CCACCAGATTCTCCCACAGT	TCAAGGGGTTGTTGGTCTTC
Kcna4	ATAGGAACCGTCCCAGCTTT	GCCCTGTCCTCCTCTTCTCT
Cyclophilin	GGGAAGGTGAAAGAAGGCAT	GAGAGCAGAGATTACAGGGT

(Ratiomaster microspectrophotometer and FELIX software, Photon Technology International, PTI) as described previously [21]. Measurements were represented as percentage changes in fluorescence intensities (as an indicator of intracellular Ca^{2+} dynamics, the ratio of the fluorescence emission at 510 nm in response to 340 nm and 380 nm excitation wavelengths was used). Ca^{2+} transients were measured with field stimulation of 30 V square pulses at 0.2 Hz frequency. Performing the transient Ca^{2+} changes was carried out in Fura-2AM-loaded cardiomyocytes. 30 V square pulses at a frequency of 0.2 Hz were used to stimulate cells electrically and the transient fluorescence alterations were gathered with the PTI system. Caffeine responses were measured 20 s after stopping the field stimulation with 10 mM caffeine application to the bath [14].

Confocal Microscopy Measurements

Cardiomyocytes were loaded with a ROS indicator chloromethyl-2′,7′-dichlorodihydrofluorescein diacetate (DCFDA, 5 µM for 1-h incubation). Afterward, cells were observed with a LEICA TCS SP5 laser scanning microscope. 488 nm wavelength was applied to excite DCFDA and emission was collected at 560 nm wavelength. Photobleaching and cell damage were prevented by keeping the laser line at 4–6% of maximal intensity. To obtain maximal fluorescence intensity, cardiomyocytes were subjected to a HEPES-buffered solution supplemented with hydrogen peroxide H_2O_2 (100 µM). Calculation of the peak fluorescence changes ($\Delta F/F0$, where $\Delta F = F - F0$; F identified as local maximum elevation of fluorescence intensity over basal level, $F0$) was performed from confocal images, providing results given as percentage changes in the fluorescence intensities [12]. Cardiomyocytes were treated with SBT with 1-h incubation.

Effects of SBT exposure (1-h incubation) on pH regulations in cardiomyocytes were investigated with confocal microscopy (Leica TCS SP5) by measuring intracellular fluorescence emitted from the pH dye SNARF-2AM. Cells were loaded with 10 µmol/L dye for 20 min. 514 nm argon laser was used for exciting the pH_i dye and fluorescence emission was detected at 580 nm and 690 nm. pH_i was estimated from the ratio of emission intensities at these 2 wavelengths [22].

Experiments with Langendorff-Perfused Hearts

The rats were anesthetized with sodium pentobarbital (50 $mg \cdot kg^{-1}$, i.p., the depth of the anesthesia was observed via firm toe pinch) and then euthanized. Rapid excision of the hearts was performed and hearts were prepared for the Langendorff-perfusion apparatus, as described previously. The hearts were electrically stimulated (DCS, Harward) at 300 beats/min with 1.5-ms square waves (at twice the threshold voltage) and the coronary flow rate was maintained at 10 mL/min during the experiment [23]. Alterations in the left ventricular pressure (LVP) were observed with a water-filled latex balloon which was inserted into the left ventricle. Overall data were recorded, stored, and processed online (Model 1050BP; BIOPAC Systems, Goleta, California, USA). Time to peak (TP), left ventricular end-systolic pressure (LVESP), left ventricular end-diastolic pressure (LVEDP), and its half-relaxation time (DT50) were also measured from each pressure trace. The experiments were performed before and after 1-h incubation with SBT perfusions for all measurements.

Statistical Methods

All data are expressed as the mean ± standard error of the mean (SEM). Determination of the statistical significance was performed via paired Student's t-test when comparing two groups and 2-way ANOVA when comparing multiple groups (Instat, Graphpad Inc.). The probability level of $p < 0.05$ (significance level of 95%) was considered to indicate significant differences for all comparisons. Concentration–response curves were fitted with pCLAMP 10.0 (Axon Instruments) and software Origin 6.0.

Results

Effects of SBT on AP Parameters

Figure 1a is the representative single-cell AP trace, introducing the prolongation of APD. Figure 1b introduces a prolongation with a statistically significant manner in APD_{25} (21.587 ± 1.821 for 10^{-7} M with $p < 0.001$, 39.515 ± 3.056 for 10^{-6} M SBT with $p < 0.0001$, and 116.447 ± 5.894 for 10^{-5} M SBT with $p < 0.0001$). In terms of evaluating amplitude, Fig. 1c reveals a statistically significant reduction in a dose-dependent manner (83.375 ± 1.972 with $p < 0.01$, 79.125 ± 1.875 with $p < 0.001$, and 66.500 ± 2.619 with $p < 0.0001$ for 10^{-7}, 10^{-6}, and 10^{-5} M SBT, respectively) compared to control (90.944 ± 1.669). Figure 1d shows that significant inhibition of RMP values became pronounced only with the highest dose (-71.333 ± 2.011, compared to control -75.789 ± 0.895, with $p < 0.05$).

As shown in Fig. 1e, a significant prolongation in APD_{50} (17.024 ± 2.042 $p < 0{,}01$, 56.698 ± 7.429 with $p < 0.0001$, and 119.728 ± 6.651 with $p < 0.0001$ for 10^{-7}, 10^{-6}, and 10^{-5} M SBT, respectively) was observed compared to control (1.000 ± 4.080 for APD_{25} and 1.000 ± 3.870 for APD_{50}). Significant prolongation of APD_{90} has been observed only with 10^{-6} M SBT (64.663 ± 4.279 with $p < 0.0001$) and 10^{-5} M SBT (82.891 ± 4.550 with $p < 0.0001$) compared to control (1.000 ± 4.326) as illustrated in Fig. 1f.

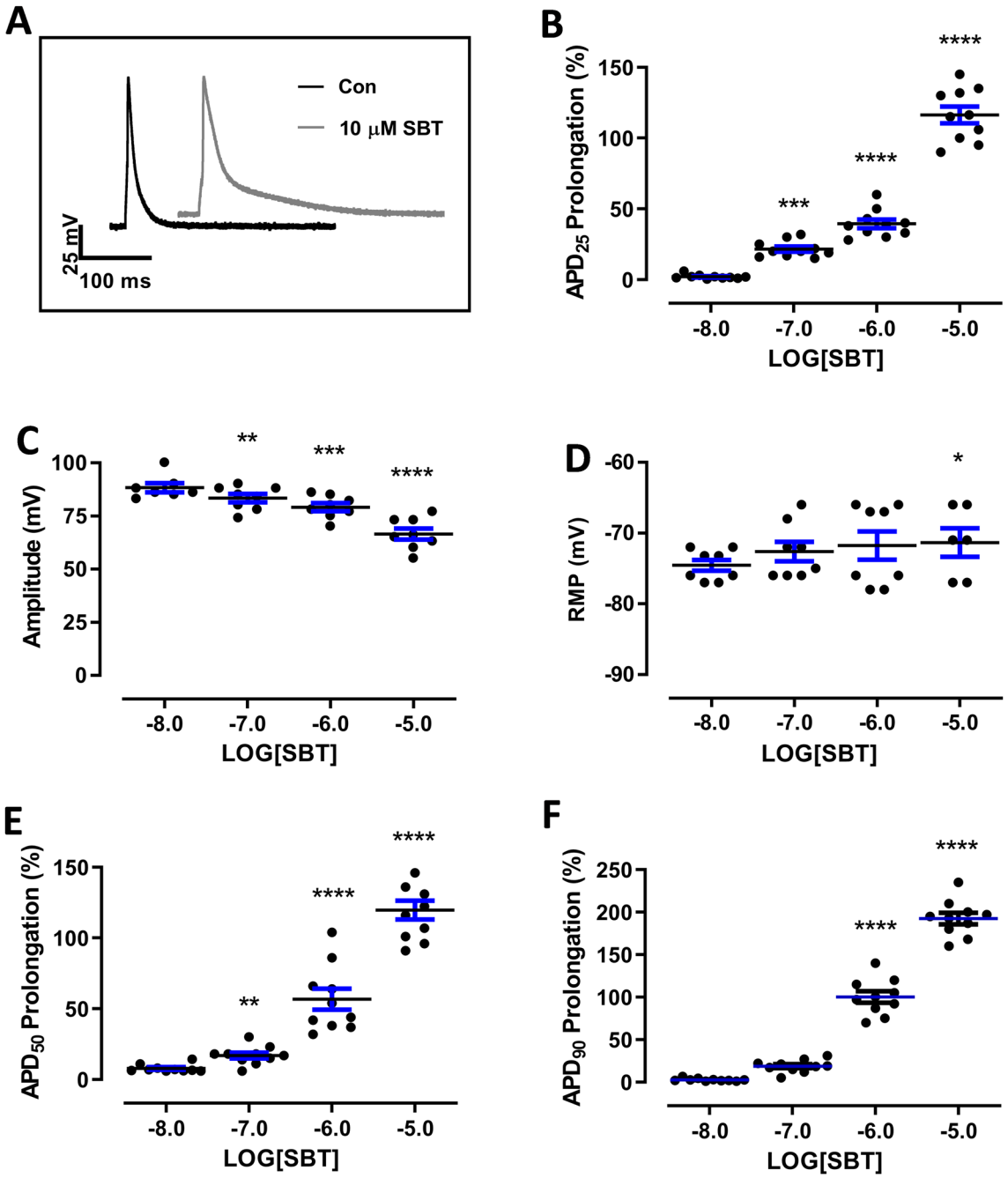

Fig. 1 Concentration-dependent manner of acute SBT treatment on action potential parameters in freshly isolated cardiomyocytes. **a** Representative single-cell action potential traces for groups is given. **b** APD_{25} percent prolongation is shown. **c** Amplitudes of AP and **d** RMP values are given. Repolarizing phases of APD of **e** 50% and **f** 90% (APD_{50} and APD_{90}) are examined following SBT treatment. Total number of cells: $n = 11–17$. Data are presented as Mean ± SEM. $^{*}p < 0.05$, $^{**}p < 0.01$, $^{***}p < 0.001$, and $^{****}p < 0.0001$ vs. Con

SBT inhibits K^+ Currents Significantly

The inhibitory effect of SBT on K^+ channel currents in ventricular myocytes is shown in Fig. 2. Figure 2a demonstrates representative K^+-channel traces. In a concentration-dependent manner, SBT inhibits (b) the rapidly activating and inactivating transient outward component, I_{to}, (c) the inward rectifier K^+ current I_{K1}, and (d) the slowly inactivating, steady-state component, I_{ss}, in cardiomyocytes. From the lowest to the highest effective doses of SBT, mean ± SEM and p values are as follows: for I_{to} 30.800 ± 7.838 with $p < 0.01$, 39.500 ± 8.547 with $p < 0.001$, and 39.500 ± 8.547 with $p < 0.001$, for I_{K1} 18.286 ± 3.018 with $p < 0.05$, 32.143 ± 3.481

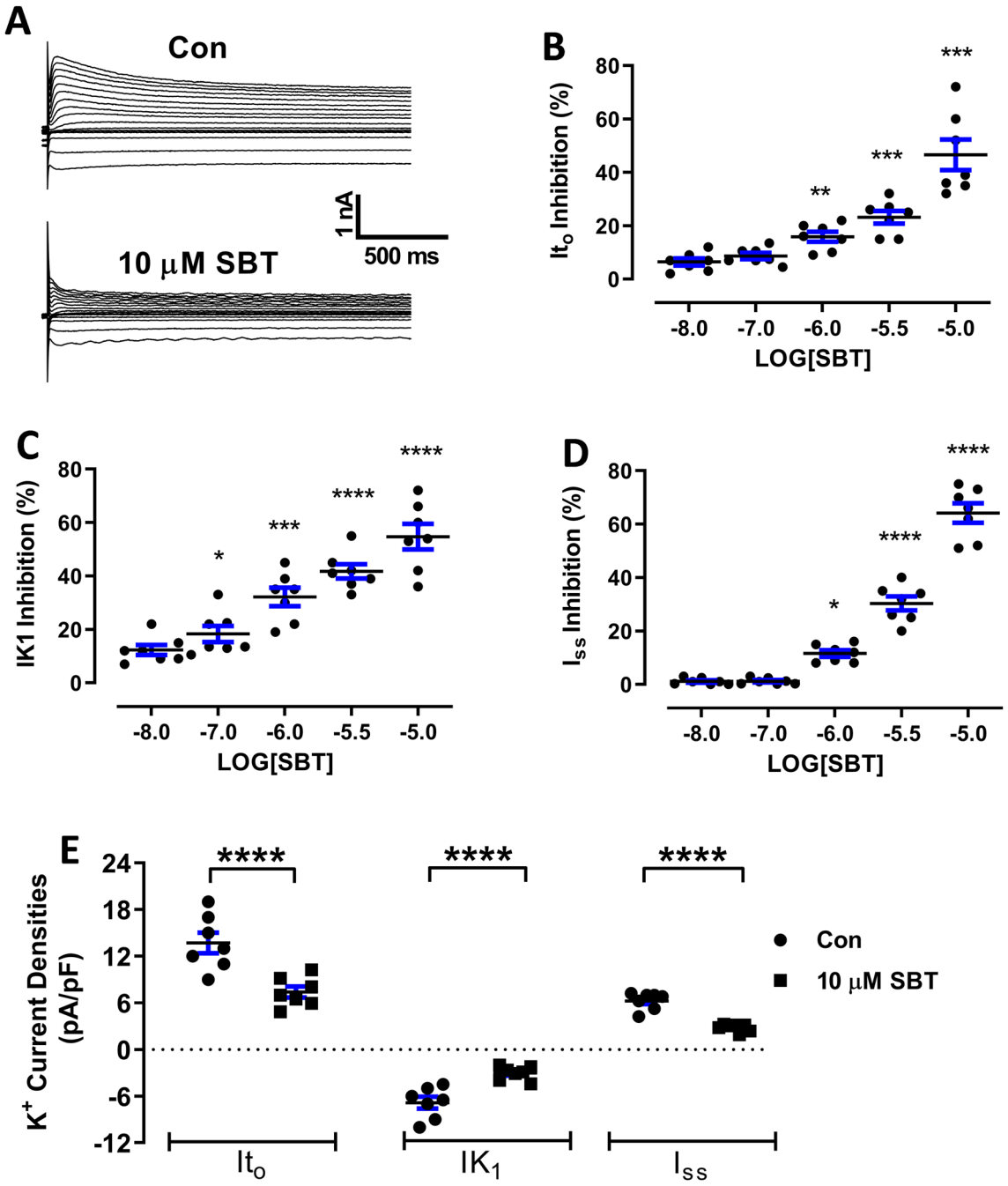

Fig. 2 Effects of acute SBT treatment on K^+-channel currents in freshly isolated cardiomyocytes. **a** Demonstration of representative K^+-channel traces for groups. **b** Concentration-dependent manner of SBT on outward K^+-channel currents (I_{to}), **c** inward rectifying K^+-channel currents (I_{K1}), and **d** steady-state K^+-channel currents (I_{ss}) in cardiomyocytes. **e** The total K^+-channel currents under 10 μM SBT treatment. Number of cells: $n = 7–10$. Significance level at $^*p < 0.05$ vs. Con

with $p < 0.001$, 41.714 ± 2.643 with $p < 0.0001$, and 41.714 ± 2.643 with $p < 0.0001$, for I_{ss} 11.571 ± 1.250 with $p < 0.01$, 50.286 ± 2.607 with $p < 0.001$, and 30.286 ± 2.607 with $p < 0.001$. Control values for I_{to}, I_{K1}, and I_{ss} are 1.000 ± 3.997, 1.000 ± 4.628, and 1.000 ± 3.691, respectively.

In Fig. 2e, the total K^+-channel current densities (pA/pF) under 10 μM SBT treatment were shown to be inhibited significantly ($p < 0.0001$).

qPCR Results on mRNA Expression Levels of K^+-Channels Support the Inhibitory Effects of SBT on K^+ Currents

The effects of SBT on K^+-channel-related mRNA expression levels were evaluated at 10 µM concentration and hence SBT was displaying statistically significant effects on electrophysiological parameters tested in this study mainly at this concentration. The mRNA levels of (Fig. 3a) fast (Kv4.2 and Kv4.3) and (Fig. 3b) slow (Kv1.4 and Kv2.1) components of K^+-channels in cell homogenates were decreased significantly with SBT pretreatment. Mean ± SEM values are 0.443 ± 0.035 vs 1.000 ± 0.028 for Kv4.2 ($p < 0.001$), 0.406 ± 0.054 vs 1.000 ± 0.057 for Kv4.3 ($p < 0.01$), 0.296 ± 0.019 vs 1.000 ± 0.06207 for Kv1.4 ($p < 0.001$), and 0.611 ± 0.040 vs 1.000 ± 0.022 for Kv2.1 ($p < 0.01$).

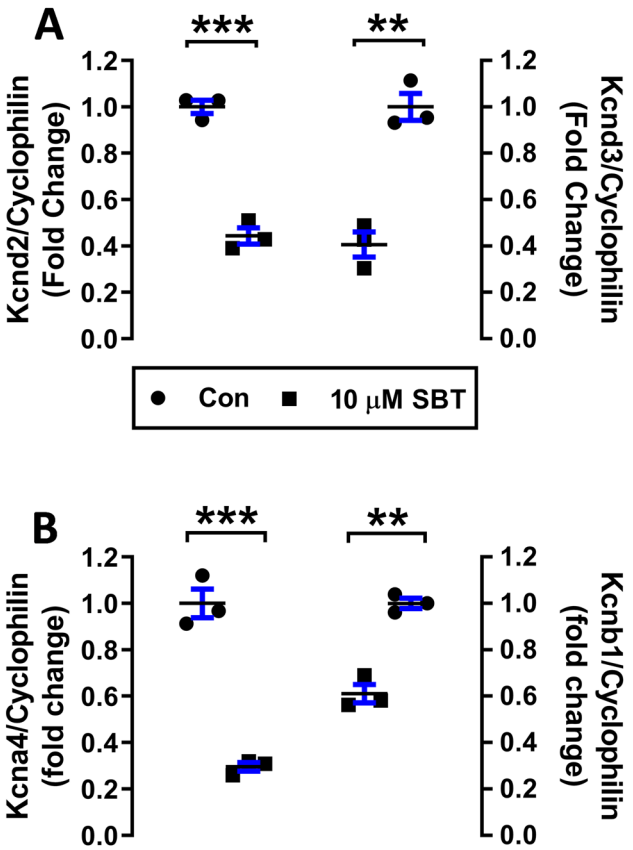

Fig. 3 The effects of chronic SBT treatment (3 h) on mRNA expression levels of K^+-channels in rat ventricular cardiomyocytes. **a** The mRNA levels of fast (Kv4.2 and Kv4.3) and **b** slow (Kv1.4 and Kv2.1) components of K^+-channels in cell homogenates. Number of replicates: 3, *$p < 0.05$ vs. Con

SBT Decreases Resting Basal Ca^{2+} While Enhancing Amplitude and Caffeine Responses Without Any Effect on Kinetic Parameters of Transients

10 µM SBT pretreatment significantly ($p < 0.01$) reduced the basal level of intracellular free Ca^{2+} in cardiomyocytes (0.315 ± 0.010, for control 0.368 ± 0.013), whereas electric-field stimulation-induced Ca^{2+} transient amplitudes were significantly ($p < 0.05$) increased in cardiomyocytes treated with only 1 µM SBT (0.236 ± 0.013) compared to control (0.198 ± 0.012) (Fig. 4b). The caffeine-induced Ca^{2+} transients, considered as an indicator of sarcoplasmic reticulum (SR) Ca^{2+} load, significantly ($p < 0.05$) enhanced in cardiomyocytes treated with 10 µM SBT (0.415 ± 0.019) compared to control (0.368 ± 0.011), as shown in Fig. 4c. As markers of kinetic parameters of transients, TP or DT50 was not affected by SBT treatment (Fig. 4d).

Confocal Imaging Represents Enhancing Effects of SBT on ROS and Inhibitory Effects on pH_i Levels

Representative images of DCFDA-loaded cardiomyocytes were intensified by H_2O_2 exposure to achieve ROS increase (Fig. 5a). Total ROS levels markedly increased following SBT treatment (145.368 ± 9.748 for 1, $p < 0.01$ and 171.643 ± 14.422 for 10 µM SBT, $p < 0.01$, for control 100.000 ± 5.765) in a concentration-dependent manner.

In Fig. 5b, representative images of ratiometric Snarf-1AM-loaded cardiomyocytes (left side) and pH_i values (right side) after SBT exposure in cardiomyocytes are given. Mean ± SEM for pH_i in control group was 0.512 ± 0.006 ($n = 78$). SBT loading significantly increased intracellular pH values to 0.543 ± 0.015 ($n = 29$, $p < 0.05$) for 1 µM and to 0.597 ± 0.017 ($n = 45$, $P < 0.0001$) for 10 µM. A difference was also detected between 10 and 1 µM SBT treatment ($p < 0.05$).

Mechanical Dysfunction is Observed in Langendorff-Perfused Hearts

The effects of SBT on systolic and diastolic pressure were evaluated at 1 and 10 µM concentration and hence it was displaying statistically significant effects on the parameters tested in this study mainly at these concentrations. Figure 6 illustrates LV pressure (systolic and diastolic) results for the control, 1 µM and 10 µM SBT-treated groups. Figure 6a represents the original experimental traces.

SBT treatment resulted in an elevation in LVEDP at 10 µM concentration (170.681 ± 16.090 vs 100.000 ± 9.609, $p < 0.01$) while it did not affect LVESP (Fig. 6b). As shown

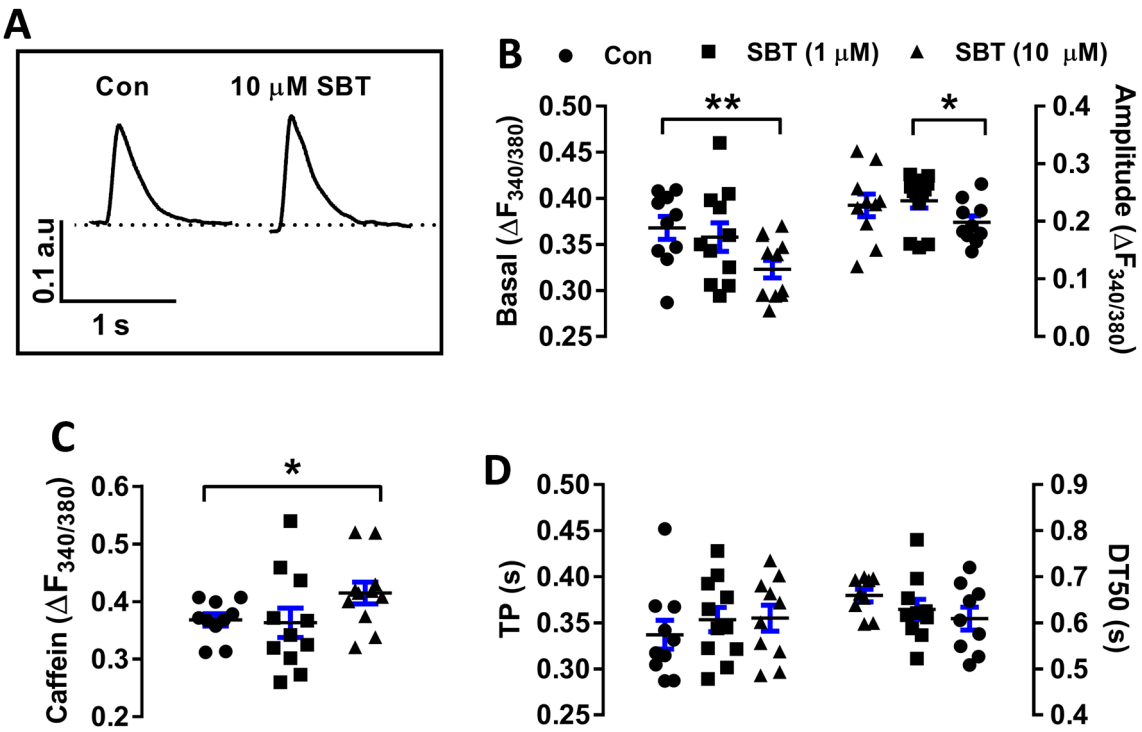

Fig. 4 Changes in Ca^{2+} transients after the acute SBT treatment in Fura-2AM-loaded cardiomyocytes. **a** Representative Ca^{2+} transients are given for groups. **b** Resting basal Ca^{2+} and amplitude of transients are given. **c** Assessment of SR Ca^{2+} content was achieved following 10 mM Caffeine treatment for SBT-treated cells. **d** Evaluation of kinetic parameters of transients such as TP and DT_{50} after SBT treatment. The total number of cells: $n = 11–15$. Significance level at $^{*}p < 0.05$ vs. Con. All data are introduced as mean (±SEM). Comparisons are carried out by the Student *t* test

in Fig. 6c, no significant effect of SBT treatment was detected on TP DT50.

Discussion

Oxidative stress plays a significant role in the pathogenesis of cardiovascular system disorders. The results observed in this study indicate that one of the mechanisms involved in the cardiotoxicity of SBT is to increase ROS levels. Elevated cellular ROS induces alterations on Ca^{2+} handling, mitochondrial functions, and gap junction remodeling, all leading to arrhythmogenesis [24]. Agents inhibiting ROS can be suggested to maximize management regarding clinical manifestations of SBT.

Scavenging ROS was found to attenuate pathological inhibition of K^+ currents. Alterations in K^+ currents have arrhythmogenic potential [12, 25]. K^+ channel mediates the main ion current of AP repolarization in ventricular myocytes [26]. The cardiomyocyte AP is the most principal component of cardiac electrophysiology and the APD is one of the prime features in AP [27]. Considering the importance of K^+ currents in AP configuration and possible effects of APD alterations in several cardiogenic pathologies, the present study was undertaken to further elucidate acute effects of SBT on APD in ventricular myocytes and contributing K^+ currents [26, 28, 29].

APD_{25} is primarily created by I_{to}, and APD_{50} is mostly created by I_{CaL} and I_K. APD_{90} is mostly affected by I_K, and partially by I_{K1} and I_{to}. An enhancement in inward currents or a reduction in outward currents can cause the prolongation of APD [26]. APD prolongation is a characteristic feature of various heart diseases in human and animal models and it is associated with ventricular arrhythmias [13]. From the findings obtained in the present study, SBT treatment was shown to induce prolongation of APD in all repolarizing levels.

To clarify the mechanism underlying the APD prolongation after SBT administration, the repolarizing K^+ currents were examined. Furthermore, because the depolarization of RMP is associated with arrhythmogenesis in acute MI, RMP values were also evaluated [30].

I_{to} current is one of the leading currents that adjust the APD of several mammalian tissues including human and rat cardiac tissues [13, 29]. I_{to} channels cloned from human and rat hearts share 98% amino acid sequence homology [31]. Even though the data presented in this study were bred from rat cardiomyocytes, the inhibitory effects of SBT on I_{to} are

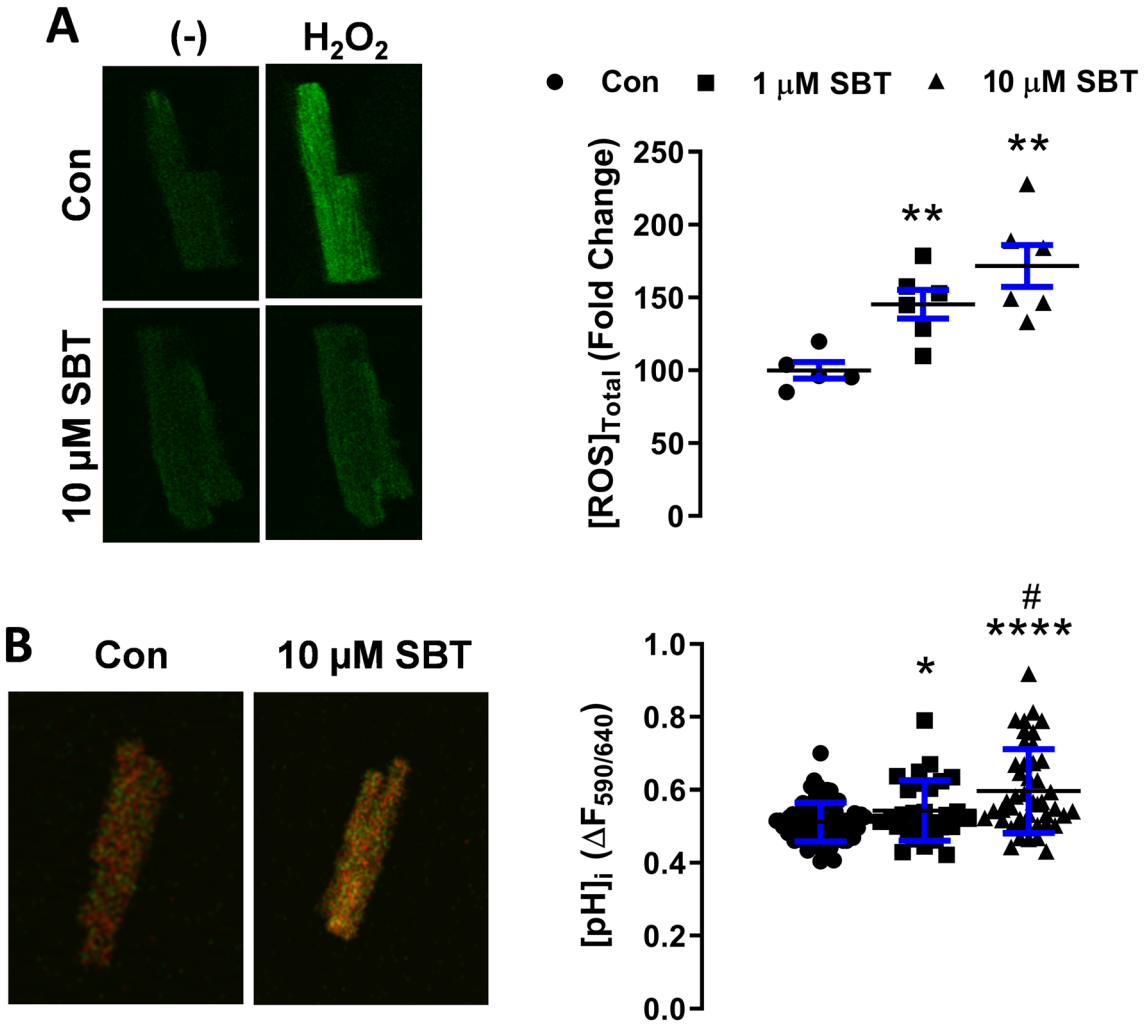

Fig. 5 Monitoring total reactive oxygen species (ROS) and H^+ concentration (pH_i) after acute SBT exposure in cardiomyocytes. **a** Representative images of DCFDA-loaded cardiomyocytes after H_2O_2 exposure (left side) and amount of ROS production (right side) following SBT exposure. **b** Representative images of Snarf-1 AM-loaded cardiomyocytes (left side) and pH_i values (right side) after acute SBT exposure in cardiomyocytes. The total number of cells: $n = 5–35$. Significance level at $^*p < 0.05$ vs. Con. $^{\#}p < 0.05$ vs. 1 μM SBT treatment

possibly similar in human ventricular cardiomyocytes. It is the main contributing current to phase 1 of AP by transiently permitting outflow of K^+ at positive membrane potentials [32, 33]. As known, I_{to} helps protect against arrhythmias. Suppression of I_{to} leads to prolongation of APD and account for positive inotropy [31].

The reduced I_{to} has been shown to cause an increase in AP amplitude [34]. An increase in peak amplitude is an indicator of a positive inotropic effect [35]. Our findings exhibited the inhibitory effect of SBT on peak amplitude values. On this basis, SBT treatment could be suggested to trigger a distinct loss of Na^+ and Ca^{2+} channel function so the inhibition of I_{to} caused by SBT treatment does not eventuate in an increase in AP amplitude. This issue will be tested in future experiments.

I_{ss} is another leading repolarizing K^+ current that regulates APD [13, 29, 31]. Suppression of I_{ss} leads to APD prolongation and prolonged QT interval, which is present in the cardiotoxicity of SBT [20, 36].

I_{K1} has inward rectifier property, plays a major role in the plateau phase of the cardiac AP, maintains the RMP by permitting outflux of K^+ at highly negative membrane potentials, and is responsible for shaping the initial depolarization and final repolarization of AP [33, 37, 38]. It controls excitability through such a way that the downregulation of I_{K1} current increases the membrane resistance in the AP phase 4, increasing the risk that a delayed afterdepolarization will generate an arrhythmia. The influence on I_{K1} can change the RMP, and increase the incidence of arrhythmias [26]. Besides, suppression of I_{K1} has been suggested to be

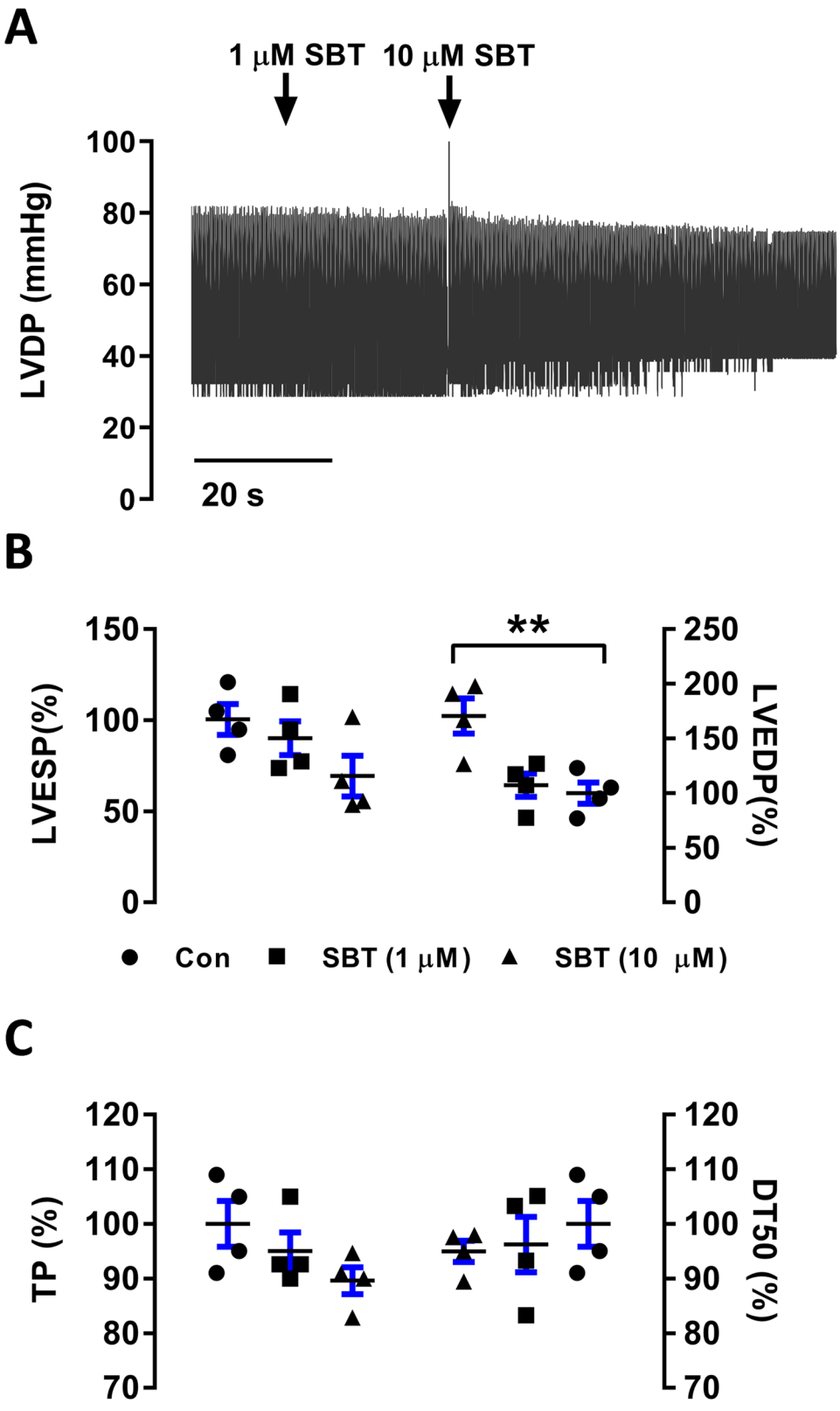

Fig. 6 Effects of SBT treatment on in vitro mechanical activity measurements of the experimental groups of hearts. **a** Experimental traces are shown in the before and after SBT treatment. **b** LVESP and LVEDP were assessed following SBT treatment in heart subjects. **c** Impact of SBT treatment on time to peak (TP) and time to half-relaxation parameters (DT50; decay time of 50%) were given. Data were presented as Mean ± SEM. The total number of hearts $N_{Heart} = 4$. *$p < 0.05$ vs Con

responsible for depolarization of RMP [37], an increase in refractoriness, and a prolongation of APD_{90}, introducing proarrhythmic effects such as causing electrical stimulated ventricular arrhythmias [38]. Depolarization of RMP, which emerges from I_{K1} inhibition, is associated with arrhythmogenesis in acute MI [26, 30, 37]. As shown in this study,

SBT inhibited I_{K1} and depolarized RMP, possibly in an interrelated manner. I_{K1}-related pathophysiologies have also been parts of the adverse effects of SBT treatment.

RMP depolarization is also associated with Na^+ channel availability [38] which may be related to cardiotoxic effects of SBT and should be studied in further researches. Besides, prolongation of all APD levels tested indicates that SBT also has effects on other ion channels for AP formation. Although further studies are needed to clarify the possible contribution of other channels and pathways to cardiotoxic effects of SBT, findings obtained here seem to have a clinical relevance for the cardiological manifestations due to illicit of this drug.

In this study, we have revealed that SBT decreased mRNA levels of different subunit I_K currents (Kv1.4, Kv2.1, Kv4.2, and Kv4.3), which are consistent with the acute effects of SBT on K^+ currents. Kv2.1 mainly forms delayed rectifier K^+ current that regulates neuronal excitability, APD, and tonic spiking [39]. Kv1.4, Kv4.2, and Kv4.3 are currents that underlie I_{to} [32], a fact that underlies the findings of this study demonstrating inhibition on this current by SBT treatment. Clinically, agents with particular effects such as a reducing effect on APD and/or a stabilizing effect on the membrane potential—favorably by facilitating the repolarizing K^+ currents—can be utilized in cardiotoxicity of SBT [40, 41]. As discussed in many previous articles [42–46], studying gene regulation of the proper cardiovascular system presents unique challenges, compared to other organ systems. As an essential organ system, environmental, pathological, and/or genetic etiologies can cause abnormal cardiac morphogenesis and disorders in the biological system function. In those regards, it has been well documented that transcriptional regulation of over thousands genes comes together to constitute a complex morphogenetic and molecular events for heart function. Cardiac transcription factors are in interaction with several co-factors and with interplay between cardiac transcription factors, *cis*-regulatory elements and chromatin as dynamic regulatory networks. Messenger RNA (mRNA) processing is an essential step for the expression of most mammalian genes. In the heart function, ion channels are critical for its proper electrical activity and any perturbation of those channels are known to cause cardiac dysfunction, such as arrhythmia. Supporting that statement, experimental studies documented that the mRNA processing defects have been shown to contribute to altered ion-channel activity and arrhythmogenesis, at most, through the mutations of the *cis*-elements within the RNA or abnormal expression of splicing factors [44–46]. Abnormal activity of cardiac ion channels has also many others causes, including amino acid sequence changes and accompanying functional abnormalities caused by genetic defects, mutations, and polymorphisms [44]. The expression level of ion channels can also be altered by dysregulation of transcription, post-transcriptional RNA processing, and protein degradation [45]. Taken into consideration our data on SBT-induced dysfunction in the voltage-dependent K^+-channel currents, and the similar changes in their mRNA levelsevidently point out the impact of human SBT treatment, particularly under the long administrations may cause higher susceptibility to arrhythmia and othertypes of cardiac complications.

Excessive ROS during myocardial oxidative stress may cause an increased ROS production (ROS-induced ROS release) associated with intracellular Ca^{2+} overload [12, 25]. Ca^{2+} uptake by SR is responsible for about 60% of diastolic Ca^{2+} extrusion in cardiomyocytes, and alterations in this process are linked to arrhythmia [10]. Interestingly, the reduced basal level of intracellular free Ca^{2+} shown in this study may indicate increased activity of Sarco(endo)plasmic reticulum Ca^{2+}-ATPase (SERCA) pumps and Na^+/Ca^{2+} exchanger. Besides, the enhanced caffeine response points out the increased SERCA activity. Finally, the enhanced SR Ca^{2+} load might have a role in the increased amplitude of electric-field stimulation-induced Ca^{2+} transients due to the elevated Ca^{2+} gradient between SR and cytosol. Overall, these data indicate that SBT may have an enhancing effect on SERCA activity and thereby Ca^{2+} reuptake to the SR lumen. Positive effects of SBT on clinical cardiovascular parameters have been reported [47]. Elevated SERCA activity has been shown to display amendatory effects in the cardiovascular system [48]. The positive clinical results may have been caused by the positive influence of SBT on SERCA to some extent. Further studies involving the evaluation of the effects of SBT on SERCA are needed to support this hypothesis. By investigating the effects of SBT derivatives on SERCA activity, candidates that have an enhancer effect on SERCA can be selected for further studies.

Alterations in pH_i have been proposed to involve in impaired cellular functions in cardiomyocytes, leading to physiological changes such as reduced contractility [9]. In this study, SBT was shown to increase intracellular pH values. The rapid onset of acidosis is a well-documented characteristic of myocardial ischemia [49]. Changes in intracellular pH can lead to acute contractile depression, alterations in Ca^{2+} signaling, and electrical arrhythmias [50]. The possible clinical outcome of this inhibitory effect of SBT on pH_i is consistent with other mechanisms observed in this study and it can be related to any effect on acid-equivalent ion transporters such as Na^+–H^+ exchange (NHE) and Na^+–HCO_3^-cotransport (NBC), mediators of acid-equivalent efflux (acid extrusion), or Cl^-–HCO_3^- exchange (anion exchange; AE) and Cl^-–OH^-exchange mediators of acid-equivalent influx (acid loading) [51]. This issue should be analyzed with further investigations to target the responsible disturbance directly in clinical management.

Excessive APD prolongation which originates from a decrease in I_{to} has been proposed to cause the cardiac systolic and diastolic mechanical dysfunction. The electrophysiological alterations would be expected to result in depressed conduction of the cardiac impulse, which would make contractile function less synchronous [27]. Also, the fact that alterations in pH_i has been proposed to involve in reduced contractility revealed the need for the assessment of mechanical dysfunction [9]. The effect of SBT on the cardiac function was assessed in isolated Langendorff-perfused hearts by measuring left ventricular pressure since this method is a valid technique to evaluate cardiac function [28, 29]. LVEDP was elevated by 10^{-5} M SBT treatment. This finding represents the aggravating effects of SBT on myocardial recovery and its negative inotropic and lusitropic effects, which leads to the reduction of contractility [28, 52]. In the management of SBT cardiotoxicity, positive inotropic and lusitropic agents do not affect APD or QT, like lipid emulsion—which also has been considered as a candidate for generic reversal of toxicity caused by an overdose of any lipophilic drug, in this case, SBT—and amrinone or combination of agents with similar effective clinical outcomes should be considered [53].

The therapeutic dose of SBT is 15 mg/day, and C_{max} was pronounced to be 2.985 ± 1.630 ng/mL [54]. Concentration which displayed statistically significant results in this study is 10 ng/mL and it is higher than the value of C_{max} reported by Kim et al. When SBT was administered at a dose of 20 mg/day, C_{max} was found to be 7.9 ± 2 ng/mL [55]. Moreover, Jain et al. reported 6.614 ± 6.449 ng/mL C_{max} values in healthy volunteers after administration of 15 mg capsule [56]. Because SBT is a prodrug, while comparing reported serum plasma concentrations with in vitro concentration of SBT alone, the clinical contribution of the active metabolites to the effects of the drug must be considered. In this respect, the difference between the plasma concentrations analyzed in certain other studies and the concentration used in this study may show no significant difference in terms of effect. Also, because some non-prescription medicines, health foods, and counterfeit drugs or slimming products involve a significant amount of SBT, overdosing is highly possible in cardiotoxic cases. Being related to the fact that a rapid increase in SBT concentration in blood has been presumed to result in rapid accumulation of SBT or its metabolites [57], the role of overdosing in cardiotoxicity profile is substantial.

According to the Hazardous Substances Data Bank (HSDB, a subset of the TOXNET database, from NIH/NLM), management of severe toxicity for SBT is generally using lidocaine and amiodarone for ventricular arrhythmia and a short-acting cardioselective agent such as esmolol for tachycardia ("Sibutramine," 2012). Considering that SBT causes APD prolongation, it is necessary to evaluate the class 1b antiarrhythmic drug phenytoin, which shortens APD, in the case of SBT cardiotoxicity. Its effectiveness at torsades de pointes and its stabilizing effect on the membrane potential by facilitating K^+ influx make magnesium sulfate another option that can be evaluated [40, 41].

In conclusion, the highlighted mechanisms of SBT cardiotoxicity and possible pharmacotherapeutic approaches discussed above can be evaluated and may assist in clinical approaches. Comprehension of the mechanisms underlying cardiotoxicity of SBT will provide more potent therapeutic approaches to cardiotoxicity cases and preclinical data to develop new agents with similar efficacy and a safer cardiovascular side effect profile. Based on the fact that preclinical cardiovascular research field testing requires improvement [58], we also emphasize the necessity to test the parameters assessed in this study for toxicity while evaluating SBT derivatives and other candidates in the treatment of obesity. Further studies are under investigation to clarify the cardiac toxicity profile of this drug.

Acknowledgments This work was supported by Anadolu University Scientific Research Projects [Grant Number 1707S448].

Compliance with Ethical Standards

Conflict of interest None declared.

Ethical Approval All experimental procedures were approved by the local ethics committee of Ankara University (Decision No: 2010-54-271) and complied with the standards of the European Community Guidelines, the Directive 2010/63/EU, on the care and use of laboratory animals.

References

1. Yun, J., Chung, E., Choi, K. H., Cho, D. H., Song, Y. J., Han, K. M., et al. (2015). Cardiovascular safety pharmacology of sibutramine. *Biomolecules & Therapeutics, 23*(4), 386.
2. Torp-Pedersen, C., Caterson, I., Coutinho, W., Finer, N., Van Gaal, L., Maggioni, A., et al. (2007). Cardiovascular responses to weight management and sibutramine in high-risk subjects: an analysis from the Scout trial. *European Heart Journal, 28*(23), 2915–2923.
3. Obert, J., Pearlman, M., Obert, L., & Chapin, S. (2017). Popular weight loss strategies: A review of four weight loss techniques. *Current Gastroenterology Reports, 19*(12), 61.
4. Puterbaugh, J. S. (2009). The emperor's tailors: the failure of the medical weight loss paradigm and its causal role in the obesity of America: I can easier teach twenty what were good to be done than to be one of the twenty to follow mine own teaching. The brain may devise laws for the blood, but a hot temper leaps o'er a colddecree. Portia, Merchant of Venice. *Diabetes, Obesity and Metabolism, 11*(6), 557–570.
5. Goncalves, F. B., Koek, M., Verhagen, H. J., Niessen, W. J., & Poldermans, D. (2011). Body-mass index, abdominal adiposity, and cardiovascular risk. *The Lancet, 378*(9787), 227.
6. Zannad, F., Gille, B., Grentzinger, A., Bruntz, J. F., Hammadi, M., Boivin, J. M., et al. (2002). Effects of sibutramine on

ventricular dimensions and heart valves in obese patients during weight reduction. *American Heart Journal, 144*(3), 508–515.
7. Bunya, N., Sawamoto, K., Uemura, S., Kyan, R., Inoue, H., Nishida, J., et al. (2017). Cardiac arrest caused by sibutramine obtained over the Internet: A case of a young woman without pre-existing cardiovascular disease successfully resuscitated using extracorporeal membrane oxygenation. *Acute Medicine & Surgery, 4*(3), 334.
8. Ferreira, G. M., Nazar, B. P., da Silva, M. R., Carriello, M. A., Freitas, S., & Appolinario, J. C. (2018). Misuse of sibutramine and bulimia nervosa: A dangerous combination. *Brazilian Journal of Psychiatry, 40*(3), 343–343.
9. Kemi, O. J., Arbo, I., Høydal, M. A., Loennechen, J. P., Wisløff, U., Smith, G. L., et al. (2006). Reduced pH and contractility in failing rat cardiomyocytes. *Acta Physiologica, 188*(3–4), 185–193.
10. Gandhi, A., Siedlecka, U., Shah, A. P., Navaratnarajah, M., Yacoub, M. H., & Terracciano, C. M. (2013). The effect of SN-6, a novel sodium-calcium exchange inhibitor, on contractility and calcium handling in isolated failing rat ventricular myocytes. *Cardiovascular Therapeutics, 31*(6), e115–e124.
11. Pu, J., Yuan, A., Shan, P., Gao, E., Wang, X., Wang, Y., et al. (2013). Cardiomyocyte-expressed farnesoid-X-receptor is a novel apoptosis mediator and contributes to myocardial ischaemia/reperfusion injury. *European Heart Journal, 34*(24), 1834–1845.
12. Tuncay, E., & Turan, B. (2016). Intracellular Zn^{2+} increase in cardiomyocytes induces both electrical and mechanical dysfunction in heart via endogenous generation of reactive nitrogen species. *Biological Trace Element Research, 169*(2), 294–302.
13. Aydemir, M., Ozturk, N., Dogan, S., Aslan, M., Olgar, Y., & Ozdemir, S. (2012). Sodium tungstate administration ameliorated diabetes-induced electrical and contractile remodeling of rat heart without normalization of hyperglycemia. *Biological Trace Element Research, 148*(2), 216–223.
14. Tuncay, E., Okatan, E. N., Vassort, G., & Turan, B. (2013). ß-blocker timolol prevents arrhythmogenic Ca^{2+} release and normalizes Ca^{2+} and Zn^{2+} dyshomeostasis in hyperglycemic rat heart. *PLoS ONE, 8*(7), e71014.
15. Volk, T., Nguyen, T. H. D., Schultz, J. H., Faulhaber, J., & Ehmke, H. (2001). Regional alterations of repolarizing K^+ currents among the left ventricular free wall of rats with ascending aortic stenosis. *The Journal of Physiology, 530*(3), 443–455.
16. Nakahiro, M., Arakawa, O., Narahashi, T., Ukai, S., Kato, Y., Nishinuma, K., et al. (1992). Dimethyl sulfoxide (DMSO) blocks GABA-induced current in rat dorsal root ganglion neurons. *Neuroscience Letters, 138*(1), 5–8.
17. Du, X., Lu, D., Daharsh, E. D., Yao, A., Dewoody, R., & Yao, J. A. (2006). Dimethyl sulfoxide effects on hERG channels expressed in HEK293 cells. *Journal of Pharmacological and Toxicological Methods, 54*(2), 164–172.
18. Hyun, S. W., Kim, B. R., Hyun, S. A., & Seo, J. W. (2017). The assessment of electrophysiological activity in human-induced pluripotent stem cell-derived cardiomyocytes exposed to dimethyl sulfoxide and ethanol by manual patch clamp and multi-electrode array system. *Journal of Pharmacological and Toxicological Methods, 87,* 93–98.
19. Ozturk, N., Olgar, Y., Aslan, M., & Ozdemir, S. (2016). Effects of magnesium supplementation on electrophysiological remodeling of cardiac myocytes in L-NAME induced hypertensive rats. *Journal of Bioenergetics and Biomembranes, 48*(4), 425–436.
20. Shimoni, Y., Ewart, H. S., & Severson, D. (1998). Type I and II models of diabetes produce different modifications of K^+ currents in rat heart: Role of insulin. *The Journal of Physiology, 507*(2), 485–496.
21. Turan, B., Désilets, M., Açan, L. N., Hotomaroglu, Ö., Vannier, C., & Vassort, G. (1996). Oxidative effects of selenite on rat ventricular contractility and Ca movements. *Cardiovascular Research, 32*(2), 351–361.
22. Bilginoglu, A., Kandilci, H. B., & Turan, B. (2013). Intracellular levels of Na^+ and TTX-sensitive Na^+ channel current in diabetic rat ventricular cardiomyocytes. *Cardiovascular Toxicology, 13*(2), 138–147.
23. Okatan, E. N., Tuncay, E., Hafez, G., & Turan, B. (2015). Profiling of cardiac β-adrenoceptor subtypes in the cardiac left ventricle of rats with metabolic syndrome: Comparison with streptozotocin-induced diabetic rats. *Canadian Journal of Physiology and Pharmacology, 93*(7), 517–525.
24. Jeong, E. M., Liu, M., Sturdy, M., Gao, G., Varghese, S. T., Sovari, A. A., et al. (2012). Metabolic stress, reactive oxygen species, and arrhythmia. *Journal of Molecular and Cellular Cardiology, 52*(2), 454–463.
25. Yin, C., Chen, Y., Wu, H., Xu, D., & Tan, W. (2017). Attenuation of ischemia/reperfusion-induced inhibition of the rapid component of delayed rectifier potassium current by Isosteviol through scavenging reactive oxygen species. *Biochimica et Biophysica Acta (BBA)-Biomembranes, 1859*(12), 2447–2453.
26. Song, Y. J., Dong, P. S., Wang, H. L., Zhu, J. H., Xing, S. Y., Han, Y. H., et al. (2013). Regulatory functions of docosahexaenoic acid on ion channels in rat ventricular myocytes. *European Review for Medical and Pharmacological Sciences, 17*(19), 2632–2638.
27. Luo, W., Jia, Y., Zheng, S., Li, Y., Han, J., & Meng, X. (2017). Changes in the action potential and transient outward potassium current in cardiomyocytes during acute cardiac rejection in rats. *Journal of Thoracic Disease, 9*(1), 129.
28. Weiss, S., Benoist, D., White, E., Teng, W., & Saint, D. A. (2010). Riluzole protects against cardiac ischaemia and reperfusion damage via block of the persistent sodium current. *British Journal of Pharmacology, 160*(5), 1072–1082.
29. Chang, G. J., Yeh, Y. H., Lin, T. P., Chang, C. J., & Chen, W. J. (2014). Electromechanical and atrial and ventricular antiarrhythmic actions of CIJ-3-2F, a novel benzyl-furoquinoline vasodilator in rat heart. *British Journal of Pharmacology, 171*(16), 3918–3937.
30. Zhai, X. W., Zhang, L., Guo, Y. F., Yang, Y., Wang, D. M., Zhang, Y., et al. (2017). The IK1/Kir2.1 channel agonist zacopride prevents and cures acute ischemic arrhythmias in the rat. *PLoS ONE, 12*(5), e0177600.
31. Chang, G. J., Wu, M. H., Wu, Y. C., & Su, M. J. (1996). Electrophysiological mechanisms for antiarrhythmic efficacy and positive inotropy of liriodenine, a natural aporphine alkaloid from Fissistigma glaucescens. *British Journal of Pharmacology, 118*(7), 1571–1583.
32. van der Heyden, M. A., Wijnhoven, T. J., & Opthof, T. (2006). Molecular aspects of adrenergic modulation of the transient outward current. *Cardiovascular Research, 71*(3), 430–442.
33. Rhoades, R. A., & Bell, D. R. (2012). *Medical physiology: Principles for clinical medicine*. Philadelphia: Lippincott Williams & Wilkins.
34. Schulte, J. S., Seidl, M. D., Nunes, F., Freese, C., Schneider, M., Schmitz, W., et al. (2012). CREB critically regulates action potential shape and duration in the adult mouse ventricle. *American Journal of Physiology-Heart and Circulatory Physiology, 302*(10), H1998–H2007.
35. Watanabe, H., Honda, Y., Deguchi, J., Yamada, T., & Bando, K. (2017). Usefulness of cardiotoxicity assessment using calcium transient in human induced pluripotent stem cell-derived cardiomyocytes. *The Journal of Toxicological Sciences, 42*(4), 519–527.
36. Ernest, D., Gershenzon, A., Corallo, C. E., & Nagappan, R. (2008). Sibutramine-associated QT interval prolongation and cardiac arrest. *Annals of Pharmacotherapy, 42*(10), 1514–1517.
37. Chang, G. J., Su, M. J., Hung, L. M., & Lee, S. S. (2002). Cardiac electrophysiologic and antiarrhythmic actions of a pavine alkaloid

derivative, O-methyl-neocaryachine, in rat heart. *British Journal of Pharmacology, 136*(3), 459–471.
38. Skarsfeldt, M. A., Carstensen, H., Skibsbye, L., Tang, C., Buhl, R., Bentzen, B. H., et al. (2016). Pharmacological inhibition of I K 1 by PA-6 in isolated rat hearts affects ventricular repolarization and refractoriness. *Physiological Report, 4*(8), e12734.
39. Misonou, H., Mohapatra, D. P., & Trimmer, J. S. (2005). Kv2.1: A voltage-gated K+ channel critical to dynamic control of neuronal excitability. *Neurotoxicology, 26*(5), 743–752.
40. Lilley, L. L., Snyder, J. S., & Collins, S. R. (2016). *Pharmacology for Canadian health care practice*. Amsterdam: Elsevier Health Sciences.
41. Thomas, S. H., & Behr, E. R. (2016). Pharmacological treatment of acquired QT prolongation and torsades de pointes. *British Journal of Clinical Pharmacology, 81*(3), 420–427.
42. Kathiriya, I. S., Nora, E. P., & Bruneau, B. G. (2015). Investigating the transcriptional control of cardiovascular development. *Circulation Research, 116*(4), 700–714.
43. Lee, T. I., & Young, R. A. (2013). Transcriptional regulation and its misregulation in disease. *Cell, 152*(6), 1237–1251.
44. Pfahnl, A. E., Viswanathan, P. C., Weiss, R., Shang, L. L., Sanyal, S., Shusterman, V., et al. (2007). A sodium channel pore mutation causing Brugada syndrome. *Heart Rhythm, 4*(1), 46–53.
45. Shang, L. L., Pfahnl, A. E., Sanyal, S., Jiao, Z., Allen, J., Banach, K., et al. (2007). Human heart failure is associated with abnormal C-terminal splicing variants in the cardiac sodium channel. *Circulation Research, 101*(11), 1146–1154.
46. Zhou, A., & Dudley, S. C., Jr. (2014). Ion channel messenger RNA processing defects and arrhythmia. *Current Biomarker Findings, 4,* 151–160.
47. Kang, J. G., & Park, C. Y. (2012). Anti-obesity drugs: A review about their effects and safety. *Diabetes & Metabolism Journal, 36*(1), 13–25.
48. Zheng, X., & Hu, S. J. (2005). Effects of simvastatin on cardiac performance and expression of sarco-plasmic reticular calcium regulatory proteins in rat heart. *Acta Pharmacologica Sinica, 26*(6), 696–704.
49. Schroeder, M. A., Swietach, P., Atherton, H. J., Gallagher, F. A., Lee, P., Radda, G. K., et al. (2009). Measuring intracellular pH in the heart using hyperpolarized carbon dioxide and bicarbonate: A 13C and 31P magnetic resonance spectroscopy study. *Cardiovascular Research, 86*(1), 82–91.
50. Lau, A. Z., Miller, J. J., & Tyler, D. J. (2017). Mapping of intracellular pH in the in vivo rodent heart using hyperpolarized [1-13C] pyruvate. *Magnetic Resonance in Medicine, 77*(5), 1810–1817.
51. Leem, C. H., Lagadic-Gossmann, D., & Vaughan-Jones, R. D. (1999). Characterization of intracellular pH regulation in the guinea-pig ventricular myocyte. *The Journal of physiology, 517*(1), 159–180.
52. Farkas, A. S., Acsai, K., Nagy, N., Tóth, A., Fülöp, F., Seprényi, G., et al. (2008). Na^+/Ca^{2+} exchanger inhibition exerts a positive inotropic effect in the rat heart, but fails to influence the contractility of the rabbit heart. *British Journal of Pharmacology, 154*(1), 93–104.
53. Bora, S., Erdoğan, M. A., Yiğittürk, G., Erbaş, O., & Parlak, İ. (2018). The effects of lipid emulsion, magnesium sulphate and metoprolol in amitriptyline-induced cardiovascular toxicity in rats. *Cardiovascular Toxicology, 18*(6), 547–556.
54. Kim, K. S., Park, S. J., Lee, H. A., Kim, D. K., & Kim, E. J. (2008). Electrophysiological safety of sibutramine HCl. *Human & Experimental Toxicology, 27*(7), 553–558.
55. Ding, L., Hao, X., Huang, X., & Zhang, S. (2003). Simultaneous determination of sibutramine and its N-desmethyl metabolites in human plasma by liquid chromatography–electrospray ionization–mass spectrometry: Method and clinical applications. *Analytica Chimica Acta, 492*(1–2), 241–248.
56. Jain, D. S., Subbaiah, G., Sanyal, M., Shrivastav, P. S., Pal, U., Ghataliya, S., et al. (2006). Liquid chromatography/electrospray ionization tandem mass spectrometry validated method for the simultaneous quantification of sibutramine and its primary and secondary amine metabolites in human plasma and its application to a bioequivalence study. *Rapid Communications in Mass Spectrometry, 20*(23), 3509–3521.
57. Kim, S. K., Lee, S. M., Yoo, S. S., Hahm, J. R., Jung, J. H., Kim, H. S., et al. (2013). Transient thyrotoxicosis from thyroiditis induced by sibutramine overdose: A case report. *Human & Experimental Toxicology, 32*(8), 890–892.
58. Peters, M. F., Lamore, S. D., Guo, L., Scott, C. W., & Kolaja, K. L. (2015). Human stem cell-derived cardiomyocytes in cellular impedance assays: bringing cardiotoxicity screening to the front line. *Cardiovascular Toxicology, 15*(2), 127–139.